Available online at www.sciencedirect.com
SCIENCE DIRECT®
Journal of Molecular Catalysis A: Chemical 221 (2004) 105–112
JOURNAL OF MOLECULAR CATALYSIS A: CHEMICAL
www.elsevier.com/locate/molcata

Active Nb_2O_5-supported nickel and nickel–copper catalysts for methane decomposition to hydrogen and filamentous carbon

Jianzhong Li, Gongxuan Lu*, Ke Li, Weiping Wang

State Key Laboratory for Oxo Synthesis and Selective Oxidation, Lanzhou Institute of Chemical Physics, Chinese Academy of Sciences, Lanzhou 730000, P.R. China

Received 23 April 2004; received in revised form 19 June 2004; accepted 22 June 2004
Available online 3 August 2004

Abstract

Production of CO-free hydrogen and filamentous carbon via methane decomposition were carried out over Nb_2O_5-supported nickel and nickel–copper catalysts in a fixed-bed-reactor at atmospheric pressure. The results indicate that Nb_2O_5 is an effective support for Ni catalysts for methane decomposition to hydrogen. The addition of Nb_2O_5 increases the yield of hydrogen and carbon capacity of high loading bimetallic Ni–Cu catalysts, and prolongs the lifetime of these catalysts in methane decomposition at high temperature. The maximal yield of hydrogen is 7274 mol H_2/mol Ni for 65Ni–25Cu–5Nb_2O_5 catalyst at 600 °C, which is one of the highest values of the catalysts for methane decomposition reported so far. TPR results show that the reduction temperature of Ni–Cu alloy is lower than that of single Ni- or Cu-supported samples and the well-crystallized Ni–Cu species is formed in bimetallic catalysts. Powder XRD results indicate that the addition of Nb_2O_5 changes the morphology in oxidized state and increases the relative intensity of Ni(1 1 1) planes in reduced state for Ni–Cu bimetallic catalysts. SEM and TEM images of used catalysts show that the surfaces of the fresh catalyst are completely covered with catalytic filamentous carbon (CFC). The "octopus" carbon and fish-bone-like filaments are formed in the induction period in methane decomposition. The filaments formed in the steady state and in the deactivation stage are very fragile to be crushed into filaments in very small sizes in length.

Keywords: Methane decomposition; Ni–Nb_2O_5; Ni–Cu–Nb_2O_5; Hydrogen production

1. Introduction

Hydrogen is a clean fuel in H_2–O_2 fuel cells. At present, hydrogen from methane is produced mainly through steam reforming (SRM) [1] or catalytic partial oxidation (CPO) [2]. In these processes, CO is inevitably formed and has to be eliminated by subsequent process in fuel cells [3]. The H_2–O_2 cells, such as proton-exchanged membrane cells, require high purity hydrogen because CO strongly poisons the anode-electrocatalysts in the cells.

Direct catalytic decomposition of methane is regarded as a potential economical method to produce hydrogen because no CO is formed in this process. Thus, hydrogen produced through methane decomposition can be supplied directly to fuel cells without any CO-removal process [4–11]. In addition, the mixture of hydrogen and methane is more effective fuel for internal combustion engines and gas turbine power plants than natural or oil gases. However, it is ineluctable that the catalysts will lose its activity due to carbon deposition and have to be regenerated with oxygen [12,13], CO_2 [14,15] or steam [16,17], which make the processes complex and difficult to avoid these residual of ppm level CO_x in the hydrogen product. Therefore, current investigations are aimed to increase the yield of hydrogen production via methane decomposition.

It was reported [5,8] that the silica-supported-Ni (Ni/SiO_2) was one of effective catalysts for the decomposition of methane. For Al_2O_3-supported catalysts, such as Ni–Al_2O_3 (10 wt.% alumina), the maximal carbon yield was about

* Corresponding author. Tel.: +86 931 4968176; fax: +86 931 4968178.
E-mail address: gxlu@ns.lzb.ac.cn (G. Lu).

1381-1169/$ – see front matter © 2004 Elsevier B.V. All rights reserved.
doi:10.1016/j.molcata.2004.06.015

145 g C/g catalyst at 550 °C [18]. The application of alloys as catalysts opens interesting routes [18,19] to increase the yield of hydrogen in methane decomposition. In addition, the introduction of second metal to catalyst may provide significant changes in the activity and selectivity. According to a number of publications, Ni–Cu–Al_2O_3 catalysts prepared by co-precipitation methods [18,20–24] are more stable for methane decomposition than Ni–Al_2O_3 catalyst. For example, the highest yields of carbon (Y_C) reported are 675 g C/g Ni (grams of carbon accumulated on per gram of Ni) [21] and 700 g C/g Ni [22], respectively.

Niobium oxide, due to its considerable acidity, has been used as a support for bi-functional catalysts [25–28]. In the present work, we studied the decomposition of methane over Ni catalysts on various supports, and found that Nb_2O_5 was one of effective supports for Ni catalysts in methane decomposition, besides SiO_2. The addition of Nb_2O_5 could increase the hydrogen yield and carbon capacity of high-loading bimetallic Ni–Cu catalysts, and prolong the lifetime of them in methane decomposition at high temperature. The accumulated total yield of hydrogen (Y_H) reaches a maximum of 7274 mol H_2/mol Ni (moles of hydrogen produced on per mol of Ni), i.e. the Y_C reaches a maximum of 743 g C/g Ni for 65Ni–25Cu–5Nb_2O_5, which is one of the highest values among those catalysts reported so far.

During the past decades carbon materials have attracted increasing interest of scientists and technologists. The family of catalytic filamentous carbon encompasses novel materials produced by the decomposition of carbon-containing gases. CFC was the subject of numerous studies (for example, the works by Baker [29], Rostrup-Nielsen and coworkers [30], Avdeeva and coworkers [18,22]) due to its unique structure and properties. In our research, the purity of carbon (mainly CFC) formed over 65Ni–25Cu–5Nb_2O_5 after methane decomposition is above 99.5 wt.% before purification (removal of Ni, Cu and Nb_2O_5), this kind of carbon will be potentially used for the structural reinforcement applications, such as a catalyst support and adsorbent [31,32].

2. Experimental

2.1. Catalyst preparation

Methods of preparing various supported single Ni component catalysts are given in Table 1. The mixture was dried at 100 °C for 24 h. Ni–Cu alloy and Ni–Cu–Nb_2O_5 catalysts (molar ratio are shown for all Ni–Cu samples) were prepared as follows: (1) adding Nb_2O_5 to a solution of $Ni(NO_3)_2$ (0.1 g NiO/ml) and $Cu(NO_3)_2$ (0.1 g CuO/ml); (2) the mixtures of (1) were treated ultrasonically for 1 h, then by violent stirring for 6 h; (3) the residual water in the mixtures of (2) was evaporated in a rotary evaporator at 100 °C. Both Ni and Ni–Cu–Nb_2O_5 catalysts were calcined at 600 °C for 4 h, and were ground and sieved to less than 150 meshes.

2.2. Reaction

The reactions of methane decomposition were carried out in a fixed-bed quartz reactor (30 mm i.d.) under atmospheric pressure. High purity methane (99.99%) was used and 50 mg of catalyst was put in the middle part of the reactor for each run. Only hydrogen was obtained as a gaseous product in

Table 1
Methane decomposition over various supported Ni catalysts

Entry	Catalyst	Yield of carbon and hydrogen		Support
		(g C/g Ni)	(mol H_2/mol Ni)	
1	12 wt.% Ni–TiO_2[a]	354	3462	TiO_2 (P25, Degussa AG)
2	12 wt.% Ni–ZSM5[a]	12	119	ZSM5 (Si/Al = 50, LPCR, CNPC, China)
3	12 wt.% Ni–MCM22[a]	49	480	MCM22 (DICP, CAS, China)
4	12 wt.% Ni–θ-Al_2O_3[a]	132	1293	θ-Al_2O_3 (LPCR, CNPC, China)
5	12 wt.% Ni–C[a]	270	2637	Carbon fiber[d] (Homemade)
6	12 wt.% Ni–CeO_2[b]	114	1111	CeO_2
7	12 wt.% Ni–Cr_2O_3[b]	9	85	Cr_2O_3
8	12 wt.% Ni–SiO_2[b]	174	1698	SiO_2 (from silica sol with average diameter of 33nm, LPCR, CNPC, China)
9	12 wt.% Ni–Nb_2O_5[a]	377	3688	Nb_2O_5 (SCR, China)
10	5 wt.% Ni–Nb_2O_5[a]	148	1446	Nb_2O_5 (SCR, China)
11	19 wt.% Ni–Nb_2O_5[c]	393	3847	Nb_2O_5 (SCR, China)
12	32 wt.% Ni–Nb_2O_5[c]	244	2390	Nb_2O_5 (SCR, China)

Reaction conditions: 500 °C, GHSV = 24,000 ml g^{-1} h^{-1}.

[a] The catalysts were prepared by wetness impregnation of $Ni(NO_3)_2$ solution (0.1 g NiO/ml) for 6 h.

[b] The catalysts were prepared by co-precipitation of $Ni(NO_3)_2$ solution (0.1 g NiO/ml) and nitrate solution of Ce or Cr with Na_2CO_3 solution at pH value of 7, then Na^+ was washed completely; 12 wt.% Ni–SiO_2 catalyst was prepared by co-precipitation of $Ni(NO_3)_2$ solution and silica sol (25 wt.% SiO_2) at pH value of 7.

[c] The catalysts were prepared by wetness impregnation of $Ni(NO_3)_2$ solution (0.1 g NiO/ml) for 4 h, and then stirred vigorously for 6 h. Finally, the residual water in the mixtures was evaporated in a rotary evaporator at 100 °C.

[d] Carbon fiber was formed via purity methane decomposition over entry 8 at 500 °C at a GHSV of 24,000 ml g^{-1} h^{-1} till the catalyst deactivated completely.

all experiments. All catalysts were reduced in situ with a flow of 25% H_2/N_2 (v/v) mixture of 40 ml/ min at 650 °C for 30 min prior to the reaction, and the reactions were stopped when methane conversion decreased to less than 3%. The flow rates of CH_4, H_2 and N_2 were controlled separately with three mass flow controllers. A desiccating tube filled with 5 Å molecule sieve was placed between the exit of the reactor and the sampling valve of gas chromatography (GC) to remove the water formed during the reduction period. The product mixtures were separated by a 13x molecular sieve column and then analyzed on a GC equipped with a thermal-conductivity detector (TCD) using high purity Ar (99.99%) as the carrier gas.

2.3. Characterization of the catalyst and deposited carbon

H_2-TPR experiments were carried out in another fixed-bed quartz reactor (5 mm i.d.) to characterize the reduction behavior of the catalysts. Catalysts (20 mg, diluted by 30 mg quartz chips) were pretreated at 700 °C in a high purity Ar flow stream of 20 ml/min until no signals were observed. When the apparatus were cooled down to 100 °C, the carrier gas was switched to a flow of 4% H_2/Ar (v/v) mixture of 40 ml/ min, and the temperature was programmed from 100 to 700 °C at a rate of 10 °C/ min. The amounts of H_2 consumed were measured using a TCD and the signals were described on a recorder.

The XRD phase analysis was carried out by on a Rigaku D/MAX-RB X-ray diffractometer with Cu Kα radiation and a Ni filter using a scanning angle (2θ) range of 20°–80° at a scanning speed of 4°/ min.

TEM and SEM images of samples were obtained on a JEOL-1200EX transmission electron microscope operating at 80 kV and a JOEL JSM-5600LV scanning electron microscope, respectively.

3. Results

3.1. Ni–Nb_2O_5 catalysts

Yields of hydrogen and carbon from methane decomposition over various supported Ni catalysts are summarized in Table 1, with a gas hourly space velocity (GHSV) of 24,000 ml g^{-1} h^{-1} at 500 °C. Table 1 shows that different types of supported Ni catalysts possess different hydrogen yield in methane decomposition. Among all of the supported 12 wt.% Ni catalysts (entry 1 to entry 9), 12 wt.% Ni–Nb_2O_5 (entry 9) and 12 wt.% Ni–TiO_2 (entry 1) reveal high hydrogen yield and carbon capacity in methane decomposition, and give the Y_H value of 3688 and 3462 mol H_2/ mol Ni, respectively.

Fig. 1 depicts the kinetic curves of methane conversion over various Ni–Nb_2O_5 catalysts at 500 °C. Methane conversion of 5 wt.% Ni–Nb_2O_5 decreases very quickly after reaching the maximum due to low Ni content. The maximal conversion of methane and the lifetime of catalyst increase with the increase of Ni loading from 5 to 19 wt.%. The samples of 19 wt.% Ni–Nb_2O_5 and 32 wt.% Ni–Nb_2O_5 have the similar methane conversion. However, when the Ni loading reaches about 54 wt.%, the catalyst does not show obvious activity for methane decomposition. 19 wt.% Ni–Nb_2O_5 shows the highest Y_H value of 3847 mol H_2/mol Ni (equal to 393 g C/g Ni), which indicate that Nb_2O_5 is an excellent support of Ni catalysts for methane decomposition, besides SiO_2.

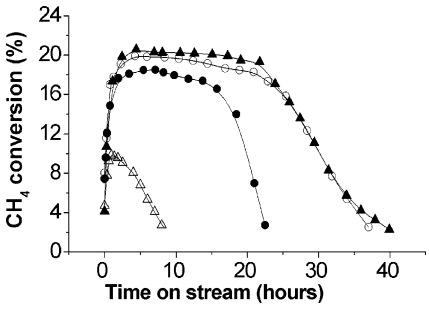

Fig. 1. Kinetic curves of methane conversion over various Ni–Nb_2O_5 catalysts at 500 °C with a GHSV of 24,000 ml g^{-1} h^{-1}: (△) 5 wt.% Ni–Nb_2O_5, (●) 12 wt.% Ni–Nb_2O_5, (◯) 19 wt.% Ni–Nb_2O_5, (▲) 32 wt.% Ni–Nb_2O_5.

3.2. Ni–Cu–Nb_2O_5 catalysts

3.2.1. Characterization of catalysts

XRD patterns of different samples (65Ni–25Cu, 65Ni–25Cu–5Nb_2O_5, and 65Ni–25Cu–10Nb_2O_5) in the oxidized and reduced states are shown in Fig. 2. Fig. 2A (oxidized state) shows the characteristic peaks of NiO and Nb_2O_5 obviously, but the characteristic peaks of copper oxide are very weak, even if its content is larger than that of Nb_2O_5. It is interesting to note that the addition of Nb_2O_5 can change the morphology of the Ni–Cu catalysts, and the relative intensity ratio of NiO(1 1 1) and (2 0 0) planes increases with the increase of Nb_2O_5 content. In Fig. 2B (reduced state), only the characteristic peaks Ni are presented, but the characteristic peaks of Cu are not observed obviously. It can be seen that the relative intensity ratio of Ni(1 1 1) and (2 0 0) planes of 65Ni–25Cu–5Nb_2O_5 is the largest among three reduced samples.

Fig. 3 illustrates the TPR curves of the Ni–Cu–Nb_2O_5 catalysts with various Ni–Cu ratios. The curves show that the samples 1–4 exhibit a similar peak and their reduction curve reaches the maximum in the range of 390–410 °C, and this process ends at near 490 °C. The reduction curve of 85Ni–5Cu–10Nb_2O_5 (sample 5) reaches a maximum in the range of 430–450 °C, which is higher than those of high Cu loading catalysts (samples 1–4). TPR curves of 23 wt.% Cu/Nb_2O_5 (sample 6) and 32 wt.% Ni/Nb_2O_5 (sample 7) are also given in Fig. 3. It can be seen that CuO was reduced between 410 and 490 °C, with a maximum at about 450 °C; while NiO is reduced between 440 and 600 °C, with

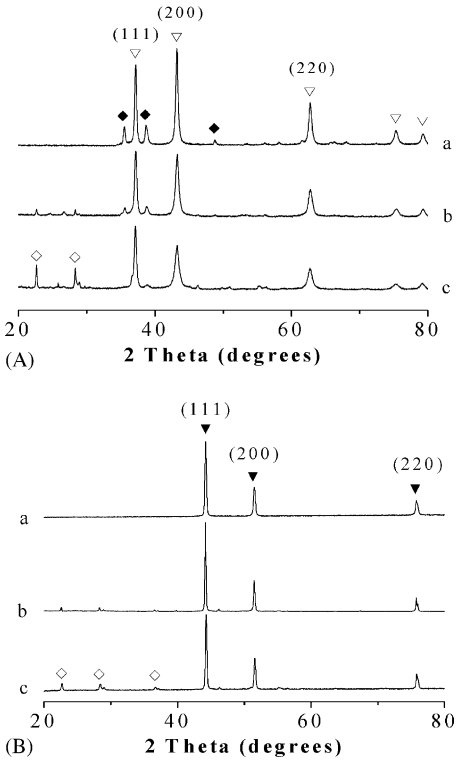

Fig. 2. XRD patterns of fresh (A) and reduced (B) catalysts: (a) 65Ni–25Cu, (b) 65Ni–25Cu–5Nb_2O_5, (c) 65Ni–25Cu–10Nb_2O_5. (◇) Nb_2O_5, (▽) NiO, (♦) CuO, (▼) Ni.

a maximum at about 560 °C. The results indicate that the addition of copper results in the decrease of reduction temperature of Ni, which leads to a 120–160 °C shift of the reduction profile of Ni to lower temperature. The incorporation of copper to the mixed oxides gives only one reduction peak, which is different from that of Feitknecht Compound (Ni–Cu–Al_2O_3) [20]. The results show that the well-crystallized Ni–Cu species is formed in bimetallic catalysts. It is reasonable to assume that Nb_2O_5 plays an important role for the composite catalysts to keep the well-crystallized phase of Ni–Cu catalysts and to enhance the hydrogen mobility on alloy.

3.2.2. Reaction

During the reactions, we have found that the Ni-supported catalyst, such as 19 wt.% Ni–Nb_2O_5, loses its activity at 600 °C within 1 h (not shown). Moreover, Ni catalyst supported on Nb_2O_5 with high loading (54 wt.%) does not show obvious activity for methane decomposition, which is different from those of the high Ni loading SiO_2- and Al_2O_3-supported catalysts [4,18]. Fig. 4 gives the yield of hydrogen over Ni–Cu–Nb_2O_5 catalysts with various Ni–Cu ratios at 500 °C with a GHSV of 24,000 ml g^{-1} h^{-1}. The 85Ni–5Cu–10Nb_2O_5 shows very low Y_H value due to low Cu introduced. However, the Y_H value improves significantly for the other four catalysts, where Cu ratio changes from 15 to 45. 65Ni–25Cu–10Nb_2O_5 has the highest Y_H value of about 3319 mol H_2/mol Ni among the five catalysts.

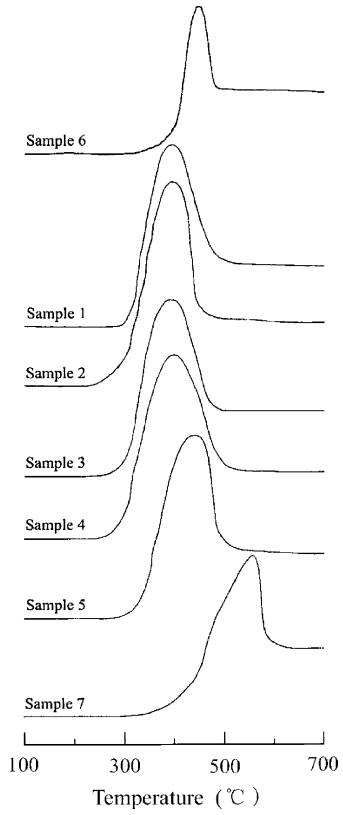

Fig. 3. H_2-TPR profiles of catalysts after calcined at 600 °C: (sample 1) 45Ni–45Cu–10Nb_2O_5, (sample 2) 55Ni–35Cu–10Nb_2O_5, (sample 3) 65Ni–25Cu–10Nb_2O_5, (sample 4) 75Ni–15Cu–10Nb_2O_5, (sample 5) 85Ni–5Cu–10Nb_2O_5, (sample 6) 23 wt.% Cu/Nb_2O_5, (sample 7) 32 wt.% Ni/Nb_2O_5.

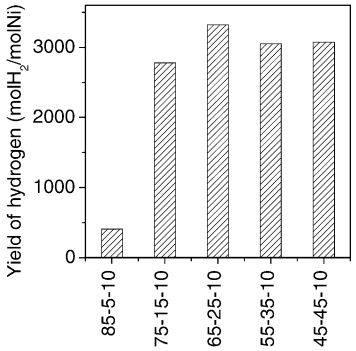

Fig. 4. Yield of hydrogen over Ni–Cu–Nb_2O_5 catalysts with various Ni/Cu ratios at 500 °C.

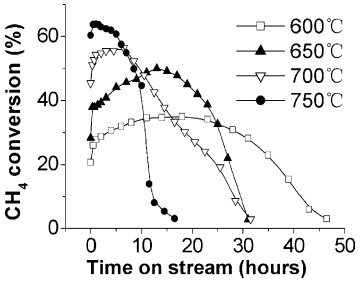

Fig. 5. Methane conversion vs. time on stream over 65Ni–25Cu–10Nb_2O_5 at 600–750 °C with a GHSV of 48,000 ml g^{-1} h^{-1}.

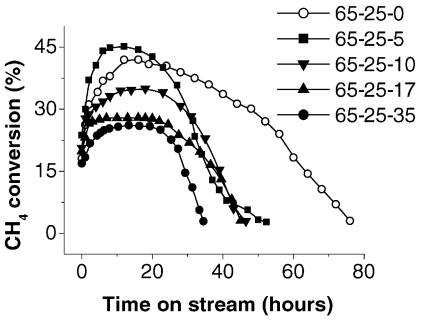

Fig. 6. Effect of Nb_2O_5 addition on methane decomposition over 65Ni–25Cu catalyst at 600 °C: (hollow symbol) GHSV = 24,000 ml g^{-1} h^{-1}; (solid symbols) GHSV = 48,000 ml g^{-1} h^{-1}.

Fig. 5 depicts the changes of methane conversion with time on stream at 600–750 °C over 65Ni–25Cu–10Nb_2O_5 catalyst. The maximal conversion of methane at 600, 650, 700 and 750 °C are 34.6, 50.0, 56.4 and 63.7%, respectively, increasing with the increase of reaction temperature. The corresponding Y_H values are 6713, 6516, 5951 and 3528 mol H_2/mol Ni, respectively. On this catalyst, steady hydrogen yield in methane decomposition can be obtained between 600 and 700 °C. The Y_H value of 3528 mol H_2/mol Ni (i.e. 361 g C/g Ni) at 750 °C shows that Nb_2O_5 prolongs lifetime of Ni–Cu catalyst and the Y_H value is much higher than that of Ni–Cu–Al_2O_3 catalyst reported by Chen et al. at high temperature [21].

Fig. 6 shows the promoting effect of Nb_2O_5 on methane decomposition over 65Ni–25Cu catalysts. After reduction period, we found that 65Ni–25Cu alloy catalyst without adding Nb_2O_5 agglomerated to blocks. This results in that the alloy catalyst shows no catalytic activity for methane decomposition at high GHSV of 48,000 ml g^{-1} h^{-1} at 600 °C. When the space velocity decreased to 24,000 ml g^{-1} h^{-1}, it shows low activity for methane decomposition. The maximal methane conversion over this catalyst (hollow symbols) is about 42% at a GHSV of 24,000 ml g^{-1} h^{-1}, and the corresponding Y_H value is about 5052 mol H_2/mol Ni. Addition of very small amount of Nb_2O_5 to Ni–Cu catalyst (e.g. 65Ni–25Cu–5Nb_2O_5) increases the Y_H value significantly. The Y_H values of the four Ni–Cu–Nb_2O_5 catalysts (solid symbols) are 5663 mol H_2/mol Ni (65Ni–25Cu–35Nb_2O_5), 6038 mol H_2/mol Ni (65Ni–25Cu–17Nb_2O_5), 6713 mol H_2/mol Ni (65Ni–25Cu–10Nb_2O_5) and 7274 mol H_2/mol Ni (65Ni–25Cu–5Nb_2O_5), respectively, increasing with the decrease of molar ratio of Nb_2O_5. Too large addition of Nb_2O_5 will decrease the catalytic activity. 65Ni–25Cu–5Nb_2O_5 shows the highest activity, with methane conversion of 45% and Y_H value of 7274 mol H_2/ mol Ni (equal to 743 g C/ g Ni). This result is one of the highest values among those catalysts reported so far. More data of the accumulated hydrogen and carbon yields are summarized in Table 2.

Table 2
Accumulated hydrogen and carbon yields taken from various Ni–Cu–Nb_2O_5 catalysts

Catalysts	Ni (wt.%)	Cu (wt.%)	Temperature (°C)	g C/g Ni	mol H_2/mol Ni
85–5–10	61.8	3.9	500	42	407
75–15–10	54.2	11.7	500	284	2778
55–35–10	39.3	27.1	500	312	3050
45–45–10	31.9	34.6	500	314	3074
65–25–10	46.7	19.4	500	339	3319
65–25–10	46.7	19.4	600	686	6713
65–25–10	46.7	19.4	650	666	6516
65–25–10	46.7	19.4	700	608	5951
65–25–10	46.7	19.4	750	361	3528
65–25–0	55.8	23.2	600	516	5052
65–25–5	50.8	21.2	600	743	7274
65–25–17	41.9	17.5	600	617	6038
65–25–35	33.2	13.8	600	579	5663

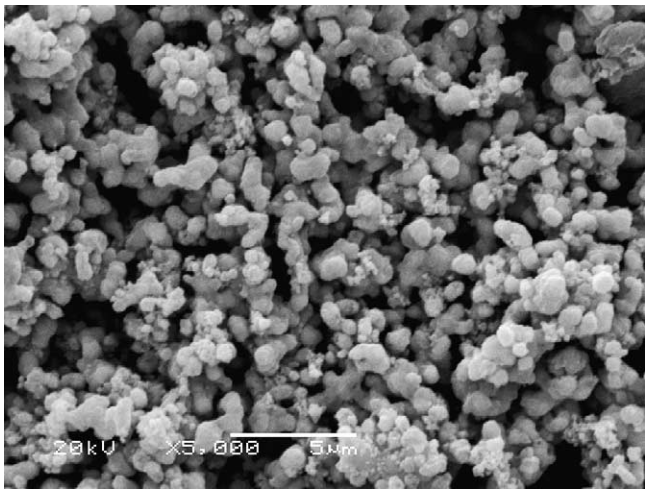

Fig. 7. SEM micrograph of fresh 65Ni–25Cu–10Nb_2O_5.

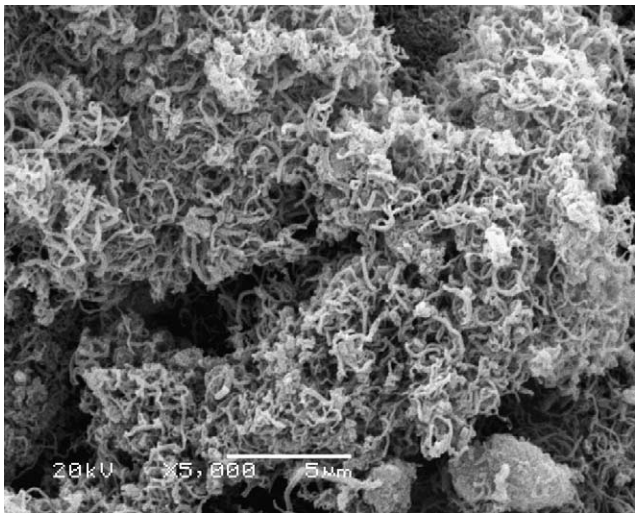

Fig. 8. SEM image of CFC formed over 65Ni–25Cu–10Nb_2O_5 at 600 °C when methane conversion is decreased to about 3%.

3.2.3. Formation of deposited carbon

The SEM image of a typical catalyst (65Ni–25Cu–$10Nb_2O_5$) is presented in Fig. 7. It can be seen that the catalyst is well mixed with particle sizes of about 1–2 μm. After methane decomposition over 65Ni–25Cu–$10Nb_2O_5$, we found that deposited carbon aggregated into blocks. The SEM image of surface carbon formed over 65Ni–25Cu–$10Nb_2O_5$ at 600 °C, till methane decomposition decreased to about 3%, is shown in Fig. 8. The image shows that the surface of catalyst is completely covered with interlaced filamentous carbon (about 50–200 nm in diameter), in contrast to the clean surfaces of the fresh catalyst (Fig. 7).

From Fig. 6, the conversion of methane can be divided into three stages: (1) the induction period, in which the methane conversion increases, is from the beginning of the reaction to about 8 h; (2) the steady state, in which the methane conversion is constant, is from about 8 h to about 24 h; (3) the deactivation stage, in which the methane conversion decreases to about 3%. TEM images of carbon formed at different stages during methane decomposition over 65Ni–25Cu–$10Nb_2O_5$ at 600 °C are shown in Fig. 9. The images show that the induction period and the steady growth of filamentous carbon occur mostly on Ni–Cu alloy particles lager than 60 nm, which are significantly larger than those of the reduced catalyst (about

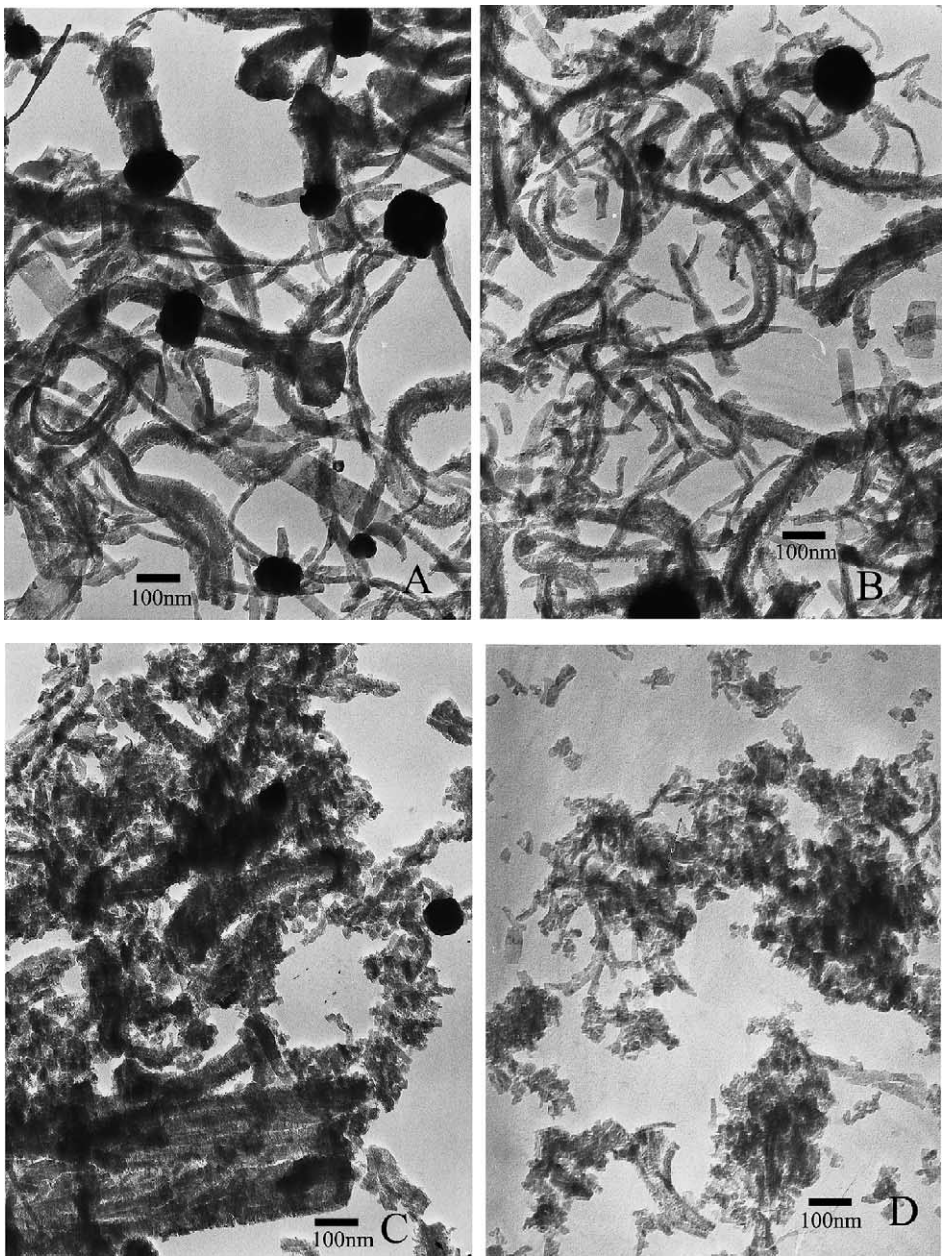

Fig. 9. TEM images of carbon formed at different stages during methane decomposition over 65Ni–25Cu–$10Nb_2O_5$ catalyst at 600 °C: methane decomposition for 20 min (A), 2 h (B) and 18 h (C), when methane conversion is decreased to about 3% (D).

25 nm) before methane decomposition. It can be seen that the quasi-octahedral particles sizes of Ni–Cu alloy are about 60–170 nm in diameter (Fig. 9A–C). In this case, several filaments grow on one particle to form the so-called "octopus" structure [20,30,33]. The diameter of the grown filaments is less than that of the metal particle. Several fish-bone-like filaments about 30–70 nm in diameter can be seen in Fig. 9B, they are the branches extended from the backbone of the filaments formed during the reaction. Comparing Fig. 9C and D with Fig. 9A,B and Fig. 8, the filaments (see Fig. 9C and D) are very fragile to be crushed into very small filaments in length. It also can be seen that some nanocarbon particles are separated from the filaments, because the samples have been treated by ultrasonic before TEM is taken.

4. Discussion

It is proposed that Ni^0 species will be separated from the support due to the growth of filamentous carbon during methane decomposition. The kinetic curves for Ni–Nb_2O_5 catalysts given in Fig. 1 are similar to the curves in [18] for the Ni catalysts, in which the induction period, the steady state period and the final period of falling activity can be seen. After the initial period of reaction, the catalyst surface structure undergoes some changes. From this moment the catalyst should be described as metal particles on the end (top) of the carbon filaments as a "living" support. These particles play catalytic role according to the generally accepted scheme [30,33].

Copper itself does not chemisorb methane and shows no activity for carbon deposition below 800 °C [34]. Copper in alloys with nickel decreases the tendency of deactivation [30]. It is also proposed that copper has a high affinity with the graphite structure and can inhibit the formation of graphite layers [29]. These effects of copper may reduce the growth rate of carbon on the nickel surface and the encapsulation of catalyst particles by carbon layers due to fast accumulation of them on nickel surface, which is regarded as the main reason of the catalyst deactivation [21]. It is found that nickel and copper tend to form alloys (see Figs. 2 and 3) over a wide composition range [35]. Incorporation of copper into the catalyst is based on the facile formation of Ni–Cu alloy, the possibility of filling the d holes of nickel by an alloying effect, and the easy donation of electrons from copper in the alloy state [20,29,33,36].

From Fig. 4, we can see that the appropriate amounts of Cu addition can increase the activity of high Ni loading catalysts. However, the catalyst with very small amounts of copper (85Ni–5Cu–10Nb_2O_5) shows poor activity for methane decomposition. The Y_H value increases with the Cu ratio increase from 5 to 25. While the Ni–Cu ratio is between 25 and 45, the Y_H value and activity of catalyst decrease because too much copper may make the catalyst particles easily become quasi-liquid and weaken their stability at high temperatures [21]. 65Ni–25Cu–10Nb_2O_5 shows the highest hydrogen yield for methane decomposition at 600 °C (see Fig. 5), which is different from that of Ni–Cu–Al_2O_3 systems reported by many investigators [20–24]. For Ni–Cu–Nb_2O_5 catalyst, the results of reactions are also in accordance with the results in reference [18,20–24]. When copper is introduced, the quantitative parameters of the reaction, such as carbon capacity and catalytic performance, change significantly at high temperature (higher than 550 °C in common). These effects of copper are pronounced due to the thorough mixing of the components during the preparation of Ni–Cu–Nb_2O_5 catalyst.

The commonly accepted model of methane decomposition and carbon growth over nickel catalysts includes the stages of activation and decomposition of methane on Ni(1 0 0) and Ni(1 1 0) planes, carbon dissolution and diffusion through the particle, carbon segregation in the form of graphite-like phase on Ni(1 1 1) planes due to crystallographic matching of Ni(1 1 1) planes to graphite(0 0 2) planes [21,33,37,38]. Thus, modifying the particle shape, one can increase the number of Ni(1 0 0) and Ni(1 1 0) planes in the catalyst active for methane decomposition, and Ni(1 1 1) planes active for carbon segregation, which in turn, increases the carbon capacity of the catalysts and decreases the deactivation rate of catalysts [22]. It has been reported that bimetallic (Rh–Co, Pd–Cu, and Pt–Sn) catalysts supported on niobia showed higher inter-metallic interaction than on alumina [27]. The addition of niobium improves the dispersion of Mo on silica [39]. Nb_2O_5 has also been used as a promoter in metal catalysts supported on SiO_2 or Al_2O_3 [40–42]. In the present study, we find that the addition of Nb_2O_5 can increase the carbon capacity of Ni–Cu catalyst for methane decomposition (see Fig. 6). From the results of Fig. 2, one can see that the addition of Nb_2O_5 can change the morphology of the Ni–Cu catalysts. 65Ni–25Cu–5Nb_2O_5 shows the largest relative intensity of Ni(1 1 1) plane among three reduced samples, which may be the reason that it gives the highest carbon capacity for methane decomposition (see Fig. 6). So Nb_2O_5 is an effective component to increase the stability of Ni–Cu bimetallic catalysts if it is added in an appropriate amount and a suitable doping way.

From Fig. 8, one can see that the surfaces of catalyst are completely covered with filamentous carbon, in contrast to the clean surfaces of the fresh catalyst (Fig. 7). The "octopus" carbon and fish-bone-like filaments (see Fig. 9A and B) are formed in the induction period. The "octopus"-type carbon was also formed over the sulfur-passivated nickel catalysts, when the sulfur coverage corresponds to ca. 70% of the saturation coverage [30]. As in the case of sulfur, formation of the "octopus"-type carbon indicates a change in the carbon nucleation when the copper concentration is above 15 wt.%, which is caused by the decrease of the carbon dissolution in nickel [20,33]. In the studies of Ni–Cu–SiO_2 catalyst by in situ XRD diffraction measurements, Alstrup and coworkers [30] found that the carbon atoms formed by the methane decomposition dissolve into the Ni particles during the induction period. This lead to the formation of large pear shaped metal particles in

the Ni catalyst and quasi-octahedral ones in the Ni–Cu catalysts. The metal particle sizes of 65Ni–25Cu–10Nb_2O_5 obtained by XRD (Fig. 2) is about 25 nm, which is smaller than that obtained by TEM (Fig. 9). These suggest polycrystalline alloy particles of catalyst are formed and only coalesced metal particles produce filamentous carbon intensively [18]. If so, one can assume that the diffusion of carbon atoms proceeds preferably on the surface of crystallites forming the catalyst particle as supposed in [30,33,43]. Thus, the surface diffusion of carbon atoms will, apparently, results in the more slight fragmentation and destruction of the particles. Introducing copper into the catalyst, the active center changes its circumstance from cubic-tetrahedral to quasi-octahedral by an increase in the number of (1 1 1) the alloy planes favorable for carbon segregation [22].

5. Conclusions

Nb_2O_5 is one of the effective supports of Ni-supported catalysts for methane decomposition to hydrogen. The addition of Nb_2O_5 increases the hydrogen yield and prolongs the lifetime of bimetallic Ni–Cu catalysts in methane decomposition at high temperature. The maximal yield of hydrogen of 7274 mol H_2/mol Ni for 65Ni–25Cu–5Nb_2O_5 at 600 °C is one of the highest values among those catalysts for methane decomposition reported so far.

The addition of Nb_2O_5 changes the morphology in oxidized state and increases the relative intensity of Ni(1 1 1) planes in reduced state for Ni–Cu bimetallic catalysts. The “octopus” carbon and fish-bone-like filaments are formed in the induction period in methane decomposition. The filamentous carbon formed in the steady state and in the deactivation stage is very fragile to be crushed into filaments in very small sizes in length. This kind of carbon will be potentially used for the structural reinforcement applications, such as a catalyst support and adsorbent.

Acknowledgements

The authors are grateful to the financial support of the “973” Project of China (TG20000264) and helpful discussions of the members in our research group.

References

[1] Z. Liu, K. Jun, H. Roh, S. Park, J. Power Sources 111 (2002) 283.
[2] S. Freni, G. Calogero, S. Cavallaro, J. Power Sources 87 (2000) 28.
[3] T. Utaka, T. Okanishi, T. Takeguchi, R. Kikuchi, K. Eguchi, Appl. Catal. A Gen. 245 (2003) 343.
[4] M.A. Ermakova, D.Yu. Ermakov, Catal. Today 77 (2002) 225.
[5] S. Takenaka, S. Kobayashi, H. Ogihara, K. Otsuka, J. Catal. 217 (2003) 79.
[6] S. Takenaka, H. Ogihara, K. Otsuka, J. Catal. 208 (2002) 54.
[7] T.V. Choudhary, C. Sivadinarayana, C.C. Chusuei, A. Klinghoffer, D.W. Goodman, J. Catal. 199 (2001) 9.
[8] S. Takenaka, H. Ogihara, I. Yamanaka, K. Otsuka, Appl. Catal. A Gen. 217 (2001) 101.
[9] M.A. Ermakova, D.Yu. Ermakov, G.G. Kuvshinov, Appl. Catal. A Gen. 201 (2000) 61.
[10] N. Shah, D. Panjala, G.P. Huffman, Energy Fuels 15 (2001) 1528.
[11] N. Muradov, Int. J. Hydrogen Energ. 26 (2001) 1165.
[12] T. Zhang, M.D. Amiridis, Appl. Catal. A Gen. 167 (1998) 161.
[13] J.I. Villacampa, C. Royo, E. Romeo, J.A. Montoya, P. Del Angel, A. Monzón, Appl. Catal. A Gen. 252 (2003) 363.
[14] M. Matsukata, T. Matsushita, K. Ueyama, Chem. Eng. Sci. 51 (1996) 2769.
[15] S. Takenaka, E. Kato, Y. Tomikubo, K. Otsuka, J. Catal. 219 (2003) 176.
[16] V.R. Choudhary, S. Banerjee, A.M. Rajput, J. Catal. 198 (2001) 136.
[17] T.V. Choudhary, D.W. Goodman, Catal. Lett. 59 (1999) 93.
[18] L.B. Avdeeva, O.V. Goncharova, D.I. Kochubey, V.I. Zaikovskii, L.M. Plyasova, B.N. Novgorodov, Sh.K. Shaikhutdinov, Appl. Catal. A Gen. 141 (1996) 117.
[19] S. Takenaka, Y. Shigeta, E. Tanabe, K. Otsuka, J. Catal. 220 (2003) 468.
[20] Y. Li, J. Chen, L. Chang, Y. Qin, J. Catal. 178 (1998) 76.
[21] J. Chen, X. Li, Y. Li, Y. Qin, Chem. Lett. 32 (2003) 424.
[22] T.V. Reshetenko, L.B. Avdeeva, Z.R. Ismagilov, A.L. Chuvilin, V.A. Ushakov, Appl. Catal. A Gen. 247 (2003) 51.
[23] Y. Li, J. Chen, Y. Qin, L. Chang, Energy Fuels 14 (2000) 1188.
[24] Y. Li, J. Chen, L. Chang, J. Zhao, Stud. Surf. Sci. Catal. 118 (1998) 321.
[25] M. Ziolek, Catal. Today 78 (2003) 47.
[26] I. Nowak, Maria Ziolek, Chem. Rev. 99 (1999) 3603.
[27] M. Schmal, D.A.G. Arandab, R.R. Soares, F.B. Noronha, A. Frydman, Catal. Today 57 (2000) 169.
[28] T. Uchijima, Catal. Today 28 (1996) 105.
[29] N.M. Rodriguez, M.S. Kim, R.T.K. Baker, J. Catal. 140 (1993) 16.
[30] C.A. Bernardo, I. Alstrup, J.R. Rostrup-Nielsen, J. Catal. 96 (1985) 517.
[31] T.V. Reshetenko, L.B. Avdeeva, Z.R. Ismagilov, V.V. Pushkarev, S.V. Cherepanova, A.L. Chuvilin, V.A. Likholobov, Carbon 41 (2003) 1605.
[32] T.V. Reshetenko, L.B. Avdeeva, Z.R. Ismagilov, A.L. Chuvilin, Carbon 42 (2004) 143.
[33] I. Alstrup, J. Catal. 109 (1988) 241.
[34] A.I. La Cava, C.A. Bernardo, D.L. Trimm, Carbon 20 (1982) 219.
[35] K.C. Khulbe, R.S. Mann, Catal. Rev. Sci. Eng. 24 (1982) 311.
[36] I. Alstrup, M.T. Tavares, J. Catal. 139 (1993) 513.
[37] F.C. Schouten, E.W. Kaleveld, G.A. Bootsma, Surf. Sci. 63 (1977) 460.
[38] F.C. Schouten, O.L. Gijzeman, G.A. Bootsma, Surf. Sci. 87 (1979) 1.
[39] S. Damyanova, L. Dimitrov, L. Petrov, P. Grange, Appl. Surf. Sci. 214 (2003) 68.
[40] F.B. Noronha, D.A.G. Aranda, A.P. Ordine, M. Schmal, Catal. Today 57 (2000) 275.
[41] M.M. Pereira, E.B. Pereira, L.Y. Lau, M. Schmal, Catal. Today 57 (2000) 291.
[42] K. Muto, N. Katada, M. Niwa, Catal. Today 35 (1999) 145.
[43] D.L. Trimm, Catal. Today 37 (1997) 233.